Weathered and unweathered surface spectra of rocks from cold deserts: identification of weathering processes and remote sensing implications

EDWARD A. CLOUTIS

GFF

Cloutis, E.A., 1992 06 10: Weathered and unweathered surface spectra of rocks from cold deserts: identification of weathering processes and remote sensing implications. *Geologiska Föreningens i Stockholm Förhandlingar,* Vol. 114, Pt. 2, pp. 181—191. Stockholm ISSN 0016-786X.

Comparisons of the reflectance spectra of weathered and unweathered surfaces of rocks from the Canadian Shield reveal that significant spectral changes can be effected by even the low weathering rates prevalent in cold desert regions. These changes include variations in overall spectral slope, the appearance/disappearance of absorption bands, shifts in absorption band minima wavelength positions, and changes in band shape. The most important alteration processes involve the oxidation of ferrous to ferric iron and the formation of hydrated mineral species. Ferric iron absorption bands are most intense for the most iron-rich lithologies. This may have important implications for the remote sensing detection of iron-rich lithologies such as iron formations and ultramafics. Aluminium- and magnesium-rich lithologies give rise to Al-OH and Mg-OH absorption bands in weathered surface spectra. Dramatic spectral variations betwen interior and exterior spectra occur even when weathered surfaces are thin enough so that underlying petrofabrics and mineralogies are still visible. □ *Canadian Shield, polar deserts, spectroscopy, weathering, remote sensing.*

Edward A. Cloutis, Department of Geology, University of Alberta, Edmonton, Alberta, Canada T6G 2E3. Present address: 4 Huntstrom Road NE, Calgary, Alberta, Canada T2K 5W3. *Manuscript received 10 July 1990, revised manuscript received and accepted 19 February 1992.*

Effective geological remote sensing of cold and polar deserts is facilitated by the fact that vegetation and soil cover is minimal. The reflectance spectra of weathered and unweathered surfaces of a number of rocks from the Canadian Shield have been measured in the laboratory in order to examine whether the low weathering rates prevalent in cold deserts are sufficient to significantly alter spectral properties. This is designed as the first step towards developing a comprehensive spectral data base for eventual quantitative geological remote sensing of cold and polar desert environments.

Geological remote sensing, while a potentially valuable technique, is limited by the fact that only the uppermost few millimeters of a rock contribute to the spectral signature. This depth is easily accessible to various physical and chemical weathering processes (Anderson & Anderson 1981; Chinn 1981). Thus, the spectral signature is strongly influenced by the surfical weathering products. This has led to the realization that the future emphasis in geological remote sensing must be on weathering alteration products (Geotz et al. 1985; Vane & Goetz 1985).

Cold desert weathering

Physical and chemical weathering operate at low rates in cold climates. The unique environment of these regions affects the relative importance of different weathering processes (Ugolini 1986). The most common alteration phenomena which have been amply documented are the formation of iron oxides/hydroxides and clays.

Cold desert weathering mobilizes and oxidizes iron. This is most evident in rust-colored staining on rock surfaces and in soils (Glazovskaya 1958; Ugolini & Bull 1965; Tedrow 1966; Ugolini 1966; Campbell & Claridge 1975; Bockheim 1979). Iron is leached from existing minerals and reprecipitated as various iron oxides and hydroxides in cracks and at the surface (Kelly & Zumberge 1961; Bardin & Konopleva 1975). Weathering rinds on rocks usually represent the minimum depth of alteration and their thickness (Anderson & Anderson 1981; Chinn 1981) routinely exceeds the depth which is accessible to spectral remote sensing (e.g. Miyamoto et al. 1981; Morris 1985).

Different ferric oxides and hydroxide are identified by their unique spectral properties: an absorption edge near 0.53 μm, (low reflectance below this

wavelength), an absorption band or shoulder near 0.64 μm, and a strong absorption band between 0.86 and 0.98 μm. These features are all due to crystal field transitions and the wavelength position of the latter band is characteristic of the particular ferric iron-bearing mineral present (Sagan et al. 1965; Sherman et al. 1982; Singer 1982; Morris et al. 1985; Sherman & Waite 1985; Townsend 1987). Studies of various ferric oxide-mineral mixtures indicate that the ferric minerals dominate the spectrum at shorter wavelengths (< 1 μm), while at longer wavelengths the other minerals are spectrally dominant (Sherman et al. 1982; Singer 1982: Singer & Roush 1983).

The formation of clays proceeds via the dissolution of various alumino-silicates in a wide range of rock types (Glazovskaya 1958; Claridge 1965; Jackson et al. 1977). Clay spectra exhibit a number of characteristic absorption bands, with bound water resulting in absorption bands near 1.4 and 1.9 μm, and structural water resulting in absorption bands near 1.4, 2.2, 2.3, and 2.4 μm. The widths, intensities and shapes of the 1.4 and 1.9 μm bands are related to the geometries of the sites occupied by the water; narrow and symmetric bands being characteristic of water molecules situated in one or a few well-ordered sites, while broad or complex bands are characteristic of disordered or multiple sites, respectively (Hunt 1977; Clark 1981). The absorption bands found near 2.2, 2.3, and 2.4 μm are combinations of a ligand-OH bend and an OH stretch. Usually only two of these three bands appear. When Al is the bonding ligand (e.g. dioctahedral clays) the bands appear near 2.2 and 2.3 μm. Mg-OH molecules (e.g. trioctahedral clays) give rise to absorption bands near 2.3 and 2.4 μm. The shorter wavelength band is usually the more intense (Hunt & Salisbury 1970; Hunt et al. 1973*a*; Hunt 1977). In general, the wavelength positions of the absorption bands are characteristic of the bonding ligand and the particular mineral (Goetz et al. 1985). The ligand-OH bands are superimposed on a reflectance dropoff towards longer wavelengths. This dropoff is the short wavelength wing of an intense fundamental OH stretching absorption near 2.7 μm which is characteristic of hydrated minerals (Hunt 1979; Roush et al. 1987). Weathered materials from cold deserts show many of the features mentioned above (Singer 1982, 1985; Agresti et al. 1986; Morris et al. 1986).

Experimental procedures

The rock samples were selected from suites of samples encompassing some important Canadian Shield rock types (R. St J. Lambert, pers. comm. 1988; Lhotka 1988). Only samples with relatively flat weathered surfaces were chosen in order to minimize phase angle effects in the spectra. Fresh surfaces were obtained by cutting the samples parallel to the weathered faces, when possible, for comparative purposes. Diffuse reflectance spectra covering the 0.35—2.6 μm range were acquired at the U.S. Geological Survey spectrometer facility in Denver, Colorado, with an average spectral resolution of 5 nm. The reflectance spectra were measured using an integrating sphere arrangement, relative to halon — a near-perfect diffuse reflector in the wavelength region of interest (Weidner & Hsia 1981), corrected for minor irregularities in halon's absolute reflectance in the 2 μm region, as well as for dark current offsets.

The spectrometer used to acquire the reflectance spectra was a Beckman 5270 double-grating, double-beam instrument that was custom interfaced to an IBM-PC computer. Spectra were measured at a signal to noise ratio of 250. Each spectrum obtained consists of the absolute reflectance and standard deviation of the mean (shown as error bars). The error bars are only shown where they are large enough that they are distinguishable from the line representing the spectrum. The Beckman spectrometer has two grating order separating filters that cross at 2.3 μm. This resulted in a low signal in this region and the frequent appearance of error bars near this wavelength. Details of the instrument and data acquisition procedurs can be found in Clark (1980) and King & Ridley (1987).

A circular area approximately 20 mm in diameter on the surface of each sample was spectrally characterized. Because of the difficulty in trying to precisely realign irregular rock faces for duplicate spectral measurements, a sample of oil sands was used to measure spectral reproducibility. The difference between duplicate measurements of this sample was found to be < 1 % across the entire wavelength region.

Sample description and spectral results

Five samples were selected with reasonably flat, lichen-free, weathered surfaces. The include a basalt (JMP2), an iron formation (5PLJ009), a volcanoclastic (4PLI017), a schist (5PLT001), and a granite (5PLJ001).

The weathered (exterior) and unweathered (interior) surfaces of the five samples have been spectrally characterized. A number of other samples were rejected because their surfaces were too angu-

lar or excessively lichen-covered. The weathered surface spectra show variable evidence of hydrated minerals, ionic mobilization, structural disruption, and oxidation of ferrous to ferric iron.

Basalt

Description. — Sample JMP2 is a basalt from the Yellowknife Bay area in the Northwest Territories (R. St J. Lambert, pers. comm. 1988). The sample is extremely fine-grained and consequently a detailed petrographic description is not possible. The interior of the sample is a uniform gray color with minor fractures, some of which are partially infilled with quartz, and some which show minor rust staining on the edges. The weathered surface is a mixture of shades of gray and brown. There is no evidence for the formation of an unconsolidated powder on the surface, suggesting that weathering has not appreciably affected the interior of this sample.

Spectral results. — A reflectance spectrum of the exterior surface was measured on a spot which was a relatively uniform gray color with no evidence of lichen. The interior spectrum was obtained on a spot which was also a uniform gray color with no visible evidence of rust staining. The reflectance spectrum of a flat, weathered surface (Fig. 1) is characterized by ferric iron absorption bands: an abrupt rise in reflectance near 0.53 μm, and two broad absorption bands near 0.65 and 0.9 μm. At longer wavelengths, an absorption feature is present near 1.4 μm and there is an additional broad, complex absorption feature between 1.85 and 2.07 μm. The reflectance maximum at 2.15 μm is followed by a reflectance decrease towards longer wavelengths with a shoulder at 2.20 μm, a sharp band at 2.25 μm, and minima at 2.32, 2.35, and 2.40 μm.

The 0.9 μm ferric iron absorption band is approximately centered at 0.88 μm, although its precise position cannot be accurately determined. The broadness of this feature is consistent with multiple, hydrated ferric iron phases such as goethite, feroxyhyte, and ferrihydrite (Sherman et al. 1982; Morris et al. 1985). Strong ferric iron absorption bands are expected in the weathering products of iron-rich materials such as basalts. The interior surface spectrum is not as strongly affected by ferric iron absorption bands as the exterior spectrum. The 0.88 μm iron absorption band is not present in the interior spectrum. Rather, a broad band is centered near 1.0 μm, which indicates that ferrous rather than ferric iron (Hunt et al. 1974; Cloutis 1985) is present in the interior spectrum. This feature is consistent with other unweathered basalt spectra (Singer & Blake 1983).

At longer wavelengths the interior and exterior surface spectra more closely resemble each other. Both display similar absorption bands near 1.4,

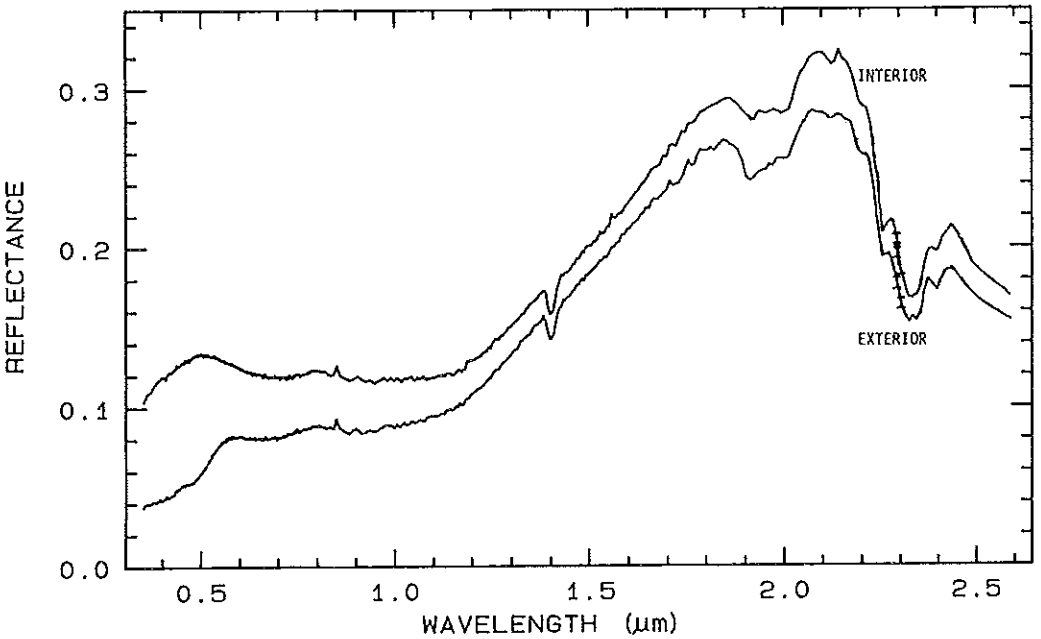

Fig. 1. Reflectance spectra of the weathered (exterior) and unweathered (interior) surfaces of a basalt (Sample No. JMP2). Error bars represent one standard deviation.

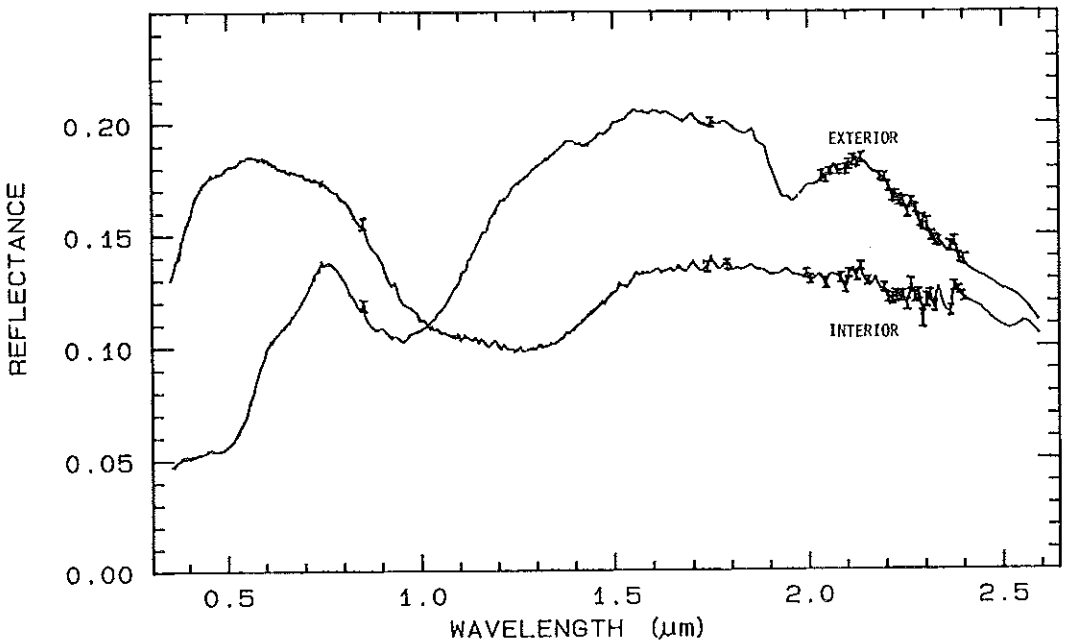

Fig. 2. Reflectance spectra of the weathered (exterior) and unweathered (interior) surfaces of an iron formation (Sample No. 5PLJ009). Error bars represent one standard deviation.

1.9—2.0, and between 2.3 and 2.6 μm. All of these bands can be attributed to various hydrated mineral phases. The bands are relatively more intense in the weathered surface spectrum. The 1.9 μm band is broad and shows a complex shape which is consistent with multiple hydrated species and/or water adsorbed onto a number of sites. Structural OH is probably present in only one or two sites in order to account for the sharpness of the 1.4 μm feature. There is also a contribution by adsorbed water to this band, although the relative abundances of the two types of water cannot be determined.

The 2.15—2.6 μm region is strongly absorbing with discrete absorption features at 2.20, 2.25, 2.32, 2.35, and 2.40 μm. Al-OH and Mg-OH bands can account for all these bands. Both Al and Mg are present in basalts, and consequently this type of spectral behavior is expected in weathered surface spectra. Although precise spectral matching is not feasible, gibbsite, chlorite and serpentine provide the best spectral matches to these bands. Overlaps and interferences of absorption bands occur in multi-component mineral mixtures (Cloutis 1985), so it is difficult to determine the relative contributions of each phase. The dropoff in reflectance beyond. 2.43 μm is probably due to the short wavelength wing of the 2.7 μm OH fundamental (Hunt 1979; Roush et al. 1987).

Iron formation

Description. — This sample (5PLJ009) is a gray and white colored, coarsely banded material consisting of magnetite, chert, and siderite (P. Lhotka, pers. comm. 1988). The sample is too fine-grained to permit a detailed petrological description but given the composition of the sample the dark bands are presumably more magnetite-rich than the light bands. Visible band widths range from a few tens of micrometers up to approximately 5 mm. The interior shows minor fracturing with variable red colored, iron staining along some of the cracks. The exterior, weathered surface is colored a deep red-brown due to ferric iron compounds. The depth of penetration of the surface staining in fracture-free areas is $<<1$ mm. The light and dark colored interior banding is partially visible through the surface coloration. This sample, and all succeeding ones, are from the Contwoyto Lake—Point Lake region in the Slave Province in the Northwest Territories (Lhotka 1988).

Spectral results. — The exterior surface spectrum was acquired on a spot which was approximately 80 % red colored and 20 % gray colored. The interior spectrum was acquired on a spot which exhibited red coloration over approximately 2 % of

the sample spot. The remainder of the spot was approximately 90 % light gray colored and 10 % dark gray colored. The interior and exterior surface spectra, measured across light and dark bands, are shown in Fig. 2. The presence of abundant iron is indicated by the appearance of the expected ferric iron spectral features in the exterior spectrum: an absorption edge near 0.53 μm, a shoulder near 0.64 μm, and a well-defined band centered near 0.95 μm. The wavelength position of the main ferric iron absorption band (near 0.95 μm) and the shape of the absorption edge and shoulder at 0.53 and 0.64 μm are most consistent with lepidocrocite and goethite (Sherman et al. 1982; Morris et al. 1985). Both minerals are hydroxides and are viable subaerial weathering products of an iron-rich assemblage. Even though the visible depth of weathering is less than a few hundred micrometers, ferrous iron and carbonate absorption bands due to the siderite are not evident. The exterior spectrum differs significantly from any of the constituent phases. Siderite has a broad absorption band extending from approximately 1.0 to 1.4 μm and strong carbonate absorption bands at 2.35 and 2.56 μm (Hunt & Salisbury 1971). Magnetie is dark and nearly featureless across the entire wavelength range (Singer 1981) but is probably contributing to the spectrum by lowering the overall reflectance. Chert (quartz) is bright and spectrally neutral and its abundance cannot be directly determined by reflectance spectroscopy in this wavelength region (Hunt & Salisbury 1970).

Weak, broad hydration bands are found near 1.42 and 1.96 μm, similar to the bands seen in goethite (Sherman et al. 1982). There are no well-defined absorption features beyound the reflectance maximum near 2.15 μm. Very weak features may be present at 2.26 and 2.37 μm. The latter band may be a highly suppressed carbonate band although other expected carbonate bands are absent. The lack of distinct Al-OH and Mg-OH absorption features is consistent whith the lack of these elements in the constituent minerals. The 2.15—2.6 μm reflectance decrease is also present in some ferric hydroxide spectra (Hovis 1965; Sagan et al. 1965) and is also seen in palagonite spectra (Singer 1982). The weakness and non-symmetric appearance of the 1.4 and 1.9 μm water bands, the absence of Al-OH and Mg-OH absorption features, and the reflectance decline beyond 2.15 μm are best explained by a structurally disordered hydrated phase. Overall, the exterior surface spectrum shows no evidence of siderite and at lower wavelengths is dominated by ferric iron features, the iron probably being derived from the siderite and/or magnetite. The shapes of the hydrated absorption bands suggest the formation of a semi-amorphous ferric iron-rich weathering product.

The interior spectrum is significantly different from the exterior spectrum. It lacks the distinctive ferric iron absorption bands at shorter wavelengths. The broad absorption band in the 1.0—1.4 μm region is characteristic of siderite, the only major constituent in the sample possessing well-defined absorption bands (Hunt & Salisbury 1971). Additional siderite bands are expected at 2.35 and 2.56 μm which should be much weaker than the 1.0—1.4 μm band. These bands are not readily apparent in the interior surface spectrum. This may again be due to the presence of magnetite which lowers overall reflectance and may partially obscure these weaker, longer wavelength bands. The interior spectrum is very similar to siderite with the additional presence of a dark, spectrally neutral phase, probably magnetite.

Volcanoclastic

Description. — Sample 4PLI017 is a felsic-pyritic metatuffite from a volcanoclastic complex in the same region as sample 5PLJ009 (above). The interior of the sample is a uniform, fine-grained mass, gray in color, with some coarse banding. The sample is extemely fine-grained and consequently a detailed petrological description is not available. A few fractures penetrate the interior and show variable amounts of iron staining. The exterior is a patchwork of gray, reddish-brown, and reddish-orange colored areas. Unfractured areas of the weathered surface show almost no visible penetration by iron staining ($<<1$ mm).

Spectral results. — The spectral measurements of the exterior surface were made on a spot which was covered by approximately 80 % brown colored and 20 % gray colored waethering products. No visible lichen was present on the spot. The interior surface which was spectrally characterized was a relatively uniform gray color with no visible evidence of rust. The interior and exterior surface spectra are shown in Fig. 3. Like the previous samples, ferric iron absorption features are expected in the exterior surface spectrum. In addition to the 0.53 and 0.64 μm features, a local minimum is found near 0.96 μm and its wavelength position is most consistent with the ferric hydroxide lepidocrocite (Sherman et al. 1982; Morris et al. 1985; Townsend 1987). The sample spectrum does not show a broad absorption band near 1.0 μm which is seen in pyrite spectra. The low reflectance of the sample may be partially responsible for this.

The absorption features at 1.4 and 1.9 μm due to

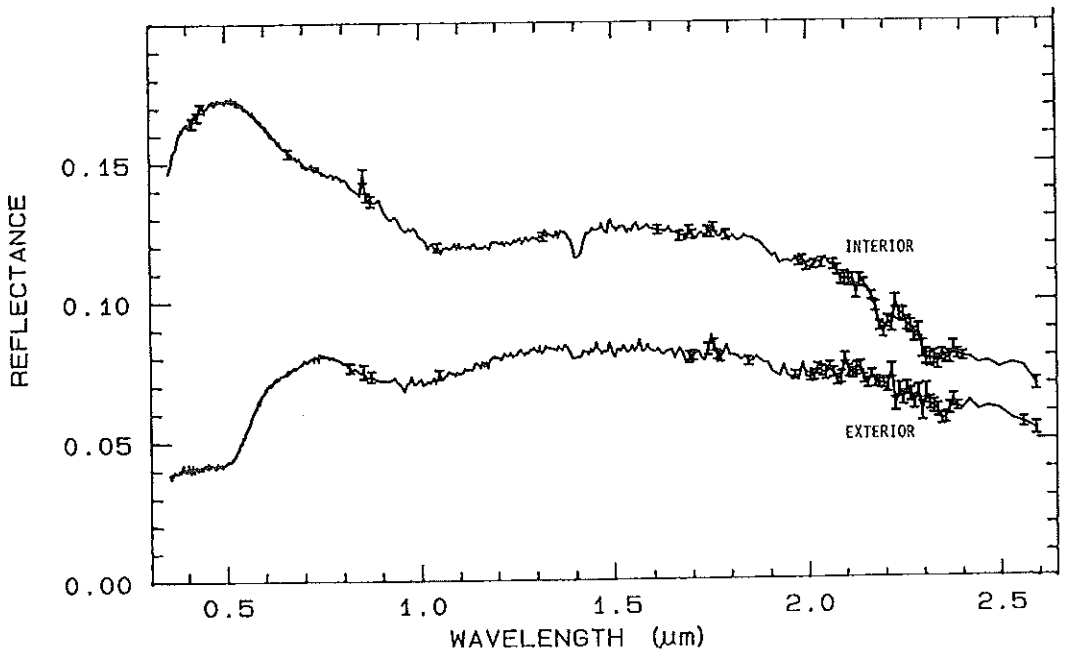

Fig. 3. Reflectance spectra of the weathered (exterior) and unweathered (exterior) surfaces of a volcanoclastic metatuff (Sample No. 4PLI017). Error bars represent one standard deviation.

hydrated minerals are weak. The broadness of the 1.9 μm band can be attributed to multiple and/or poorly crystallized phases. Lattice-OH bands are weak or absent beyond 2.15 μm. Only one absorption band at 2.34 μm is unambiguously identified. Less well-defined features may be present at 2.15, 2.22, 2.29, and 2.43 μm. Both Al-OH and Mg-OH molecules may be present in the weathered zone if these bands are real. The band at 2.15 μm, in conjunction with some of the longer wavelength features may be attributable to alunite, since sulfide oxidation is a viable weathering mechanism for the pyrite. The noise in the data is due to the low reflectance of the sample and precludes the positive identification of particular hydrated species. The lack of definable absorption bands beyond 2.15 μm is partially due to the low spectral reflectance, and may also be due to the formation of an amorphous weathering product.

The interior surface spectrum differs from the exterior in overall shape and detail. The overall slope of the former is negative while the latter is roughly flat. The interior spectrum shows no evidence for ferric iron absorption bands, although some interior weathering may be indicated by the presence of absorption bands at 1.4, 2.2 and 2.3 μm. A broad absorption band is centered near 1.05 μm which is more characteristic of ferrous rather than ferric iron, and occurs at a significantly higher wavelength than in the exterior spectrum. This band is approximately centered at the wavelength position expected for pyrite (Hunt et al. 1971; King, pers. comm. 1988). The long wavelength absorption bands at 2.2 and 2.3 μm indicate the presence of Al-OH complexes. Aluminum is readily available from the plagioclase feldspar present in the rock.

Schist

Description. — A cordierite-biotite knotted schist (5PLT001) is representative of a metamorphic sequence in the study area of Lhotka (1988). The interior of the sample shows cordierite-rich areas (containing approximately 70 % cordierite) which are enclosed by more biotite- and quartz-rich material. There are a few interior fractures which show very minor amounts of oxidized iron. The weathered surface is a light-brown color with patches of brown, gray, and orange-brown coloration. Visible alteration of the interior is again extremely limited.

Spectral results. — The spectral measurements of the exterior surface were acquired on a spot which encompassed approximately 40 % of a cordierite-rich region although the relative proportions of cordierite-rich and cordierite-poor areas could not be precisely determined due to the surface weathering. The interior spot which was spectrally characterized was composed of approximately 60 %

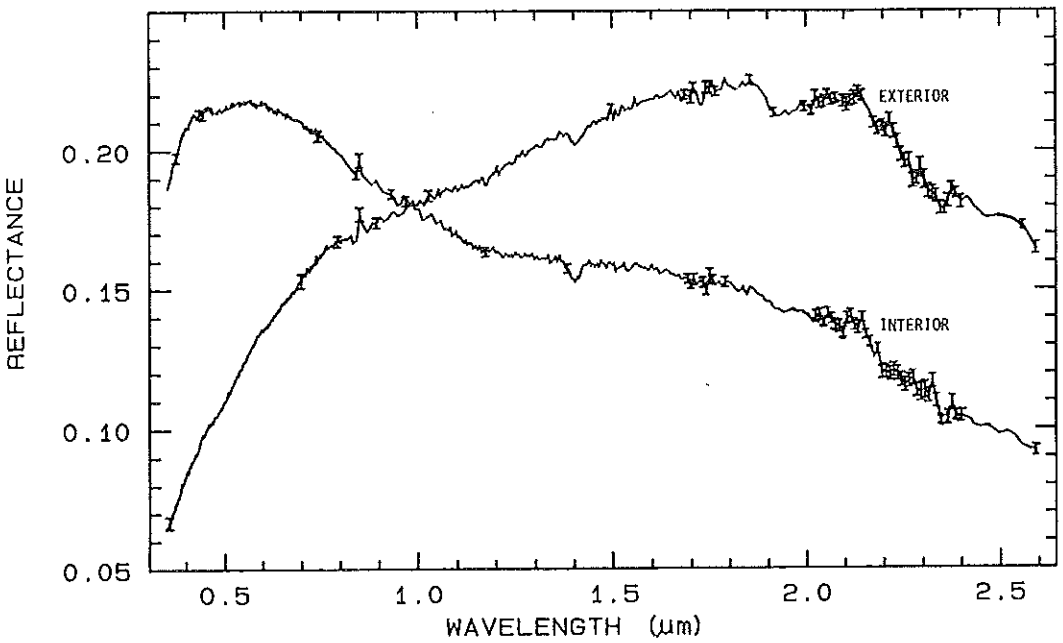

Fig. 4. Reflectance spectra of the weathered (exterior) and unweathered (interior) surfaces of a schist (Sample No. 5PLT001). Error bars represent one standard deviation.

cordierite-rich areas, 35 % cordierite-poor areas and 5 % rust colored areas. The weathered surface spectrum of this sample differs from those of the previous three by the absence of characteristic ferric iron absorption bands (Fig. 4). The sample is composed predominantly of biotite and cordierite, both of which show only weak absorption bands (Hunt & Salisbury 1970; Hunt et al. 1973*a*). There appears to be a weak band in the 1 μm region which may be due to Fe^{2+}-Fe^{3+} crystal field transitions in the weathered and unweathered species.

Broad hydroxyl bands are present near 1.4 and 1.9 μm. These band are appreciably stronger and broader than those in biotite and cordierite, suggesting that an optically significant weathered zone has been established. A local reflectance peak is present at 2.15 μm, followed by a reflectance decrease with absorption features superimposed at 2.20, 2.28, 2.36, and 2.47 μm. Assignment of these bands to specific minerals is hampered by the fact that different samples of the same mineral can have absorption bands at different wavelength positions and of different relative strengths (Hunt & Salisbury 1970; Hunt et al. 1973*a*; Hunt 1977, 1979; Clark 1981; Hunt & Evarts 1981; Hunt & Hall 1981; Goetz et al. 1985; Roush et al. 1987).

Pure cordierite is featureless in the 2.15—2.6 μm region but alters readily to muscovite (Hunt et al. 1973*a*). Biotite is only weakly featured in this spectral interval. The absorption bands seen in the sample spectrum must be due to the weathering products and include both Al-OH and Mg-OH absorption bands. Because the lattice-OH bands are not distinct, a certain degreee of disorder must be present in the weathered materials.

The interior surface spectrum is radically different from the exterior spectrum. The former displays a strong negative slope. The reason for this is unclear as neither cordiertite nor biotite have negative spectral slopes. The broad reflectance increase towards longer wavelength seen in the exterior spectrum can be attributed to charge transfers in a range of materials, and is absent from the interior spectrum. Few diagnostic absorption bands are present. Nevertheless the slope differences between the two spectra should be noted.

Granite

Description. — This foliated biotite granite (5PLJ001) is from an amphibolite grade area at Contwoyto Lake—Point Lake (Lhotka 1988). The sample is composed of approximately 55 % K-feldspar, 25 % quartz and 20 % biotite with a distinct foliated fabric. The weathered surface is a non-uniform pink-brown color. It is restricted to, at most, the outermost few 100 μm.

Spectral results. — The exterior spot which was spectrally characterized was covered with a veneer

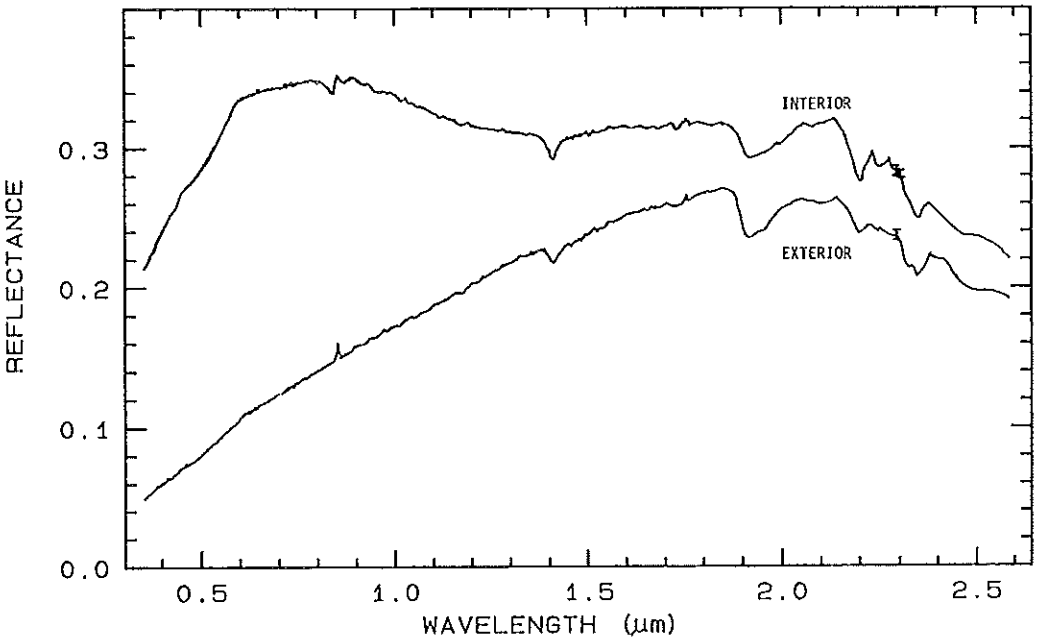

Fig. 5. Reflectance spectra of the weathered (exterior) and unweathered (interior) surfaces of a granite (Sample No. 5PLJ001). Error bars represent one standard deviation.

of pink-brown oxidation products through which the underlying mineralogy was visible. The interior spot appeared to be free of rust-colored alteration and the constituent minerals were readily apparent. The granite sample differs from the others by the lower abundance of iron-bearing minerals. This is reflected in the absence of detectable ferric iron absorption features in the exterior surface spectra (Fig. 5). The broad reflectance decline towards shorter wavelengths in the exterior spectrum is probably due to a series of charge transfers involving a number of atomic species. The inflection at 0.61 μm may be due to a very small amount of ferric iron which is derived from the weathering of the biotite. Feldspar and quartz form the bulk of the sample but are not detected in the spectrum. While quartz is spectrally featureless, feldspar often shows a broad, weak absorption band near 1.25 μm (Adams 1975) which is not evident in the exterior sample spectrum. The interior spectrum does show a weak, broad absorption band beyound 1 μm which may be attributable to the feldspar.

Asymmetric hydroxyl absorptions are present at 1.4 and 1.9 μm in both spectra. Their shape is due to multiple hydrated mineral species, a range of OH binding energies which would be present in poorly crystallized minerals, or microscopic fluid inclusions in quartz (Hunt et al. 1973*b*). Both spectra are generally similar at longer wavelengths. Al-OH absorptions can account for the bands at 2.20, 2.32, and 2.34 μm. There is no evidence for an Mg-OH absorption band at 2.4 μm, not unexpectedly, as Mg is largely absent in the sample. There is no reflectance upturn beyond 2.5 μm because of the interference of the 2.7 μm OH fundamental.

Discussion

The weathered sample spectra show many features which are inconsistent with the underlying, more pristine mineralogy. Even when the visible depth of weathering is less than a few hundred micrometers, the weathering products dominate the reflectance spectrum.

Ferric iron absorption bands dominate the low wavelength regions of the weathered spectra of the most iron-rich samples (Figs 1, 2, and 3). Ferric iron absorption bands appear in weathered surface spectra regardless of whether the iron is derived from mafic silicates (JMP2), carbonates and/or oxides (5PLJ009), or sulfides (4PLI017). This may prove to be particularly valuable for remote sensing delineation of iron-rich lithologies such as iron formations and ultramafics.

Bound and structural water bands appear in the exterior spectra, regardless of whether they are present in the interior spectra (e.g. Fig. 4). The mode of weathering can be inferred from the shape of the bands. They are frequently broad and asymmetric

and some show evidence of multiple, closely spaced, overlapping bands. Amorphous weathering products such as palagonites show broad, relatively featureless OH/H_2O absorption bands near 1.4 and 1.9 μm (Singer 1982). Each geometrically unique site in a mineral to which H_2O and OH are bonded has a unique energy of excitation. If a number of distinct sites are present, their energies will be slightly different and there will be some overlap of their bands. Such a case would result in an asymmetric absorption feature, potentially resolvable into a series of closely spaced overlapping bands.

The choice between amporhous or multiple weathering products may be inferred from the behavior of the 2.15—2.6 μm region. An intense OH fundamental band is located near 2.7 μm (Roush et al. 1987). The short wavelength wing of this feature extends into the near infrared and is at least partially responsible for the reflectance decline towards longer wavelengths. Abundant structural water and/or lattice-induced perturbations of the OH molecule should result in a broader and more intense fundamental absorption band. This in turn may cause the 2.15—2.6 μm reflectance decrease to be steeper.

The sample spectra with the most well-defined (symmetric, narrow) 1.4 μm band exhibit the most resolvable lattice-OH bands between 2.15 and 2.6 μm (samples JMP2, 5PLJ001). Broad, unstructured 1.4 μm bands bands are associated with 2.15—2.6 μm intervals showing few resolvable lattice-OH bands. The degree of crystallinity of the weathered minerals can be estimated from these parameters.

The strongest Al-OH bands appear near 2.2 and 2.3 μm, while Mg-OH bands are found near 2.3 and 2.4 μm. Mg-OH bands are most evident in the most magnesium-rich sample (JMP2), while the most aluminium- and magnesium-deficient sample (5PLJ009) is devoid of resolvable Al-OH and Mg-OH bands. The appearance of Al-OH and Mg-OH absorption bands in exterior surface spectra is also correlated with the presence of appreciable Al and Mg in the underlying lithologies. In most cases, the particular weathering products which are formed cannot, at present, be determined because of the lack of unambiguous lattice-OH absorption features and overlaps by adjacent bands.

The differences between interior and exterior spectra of the same sample range from minor to extreme. Absorption bands such as those attributable to ferric iron are often present only in the exterior surface spectra. Other absorption bands such as bound/structural water bands are of variable intensities and shapes when comparing interior and exterior spectra. Ferrous iron absorption bands seen in some interior spectra (Figs. 1, 2, and 3) are absent or have been shifted to shorter wavelengths in the exterior spectra due to the oxidation of iron to the ferric state. Overall spectral slopes can also be radically different between interior and exterior spectra. While the cause of this slope change is uncertain, it has important implications for the analysis of both broad band and narrow band remote sensing data.

Spectral studies of pristine, anhydrous minerals in the laboratory will be of little relevance to practical remote sensing of most cold and polar desert regions. Weathering rates are low in these environments but, in most cases, still significant enough to drastically alter the spectral properties of the underlying assemblages. Many of the variations seen between the interior and exterior spectra may not be amenable to analysis using spectral mixing models (e.g., Shipman & Adams 1987) because the spectral differences involve the formation of new mineral species and the destruction of existing ones.

Conclusions

The weathered surface spectra of the range of rock types considered in this study are dominanted by two classes of features. The shorter wavelength regions (< 1.3 μm) are dominated by ferric iron due to the oxidation and hydration of diverse iron-bearing minerals. These bands are most intense in the exterior spectra of the most iron-rich samples. The higher wavelength interval (> 1.3 μm) is dominated by features attributable to hydrated minerals. The shape of OH/H_2O absorption features are related to the degree of crystallinity of the weathering products. The highest wavelength regions (> 2.0 μm) are most suitable for determining the dominant ligands which are bonded to the OH molecules, in particular Mg and Al. The intensity and resolution of the 1.4 μm absorption feature correlates with the resolution of the various lattice-OH absorption bands for the samples examined.

The use of laboratory reflectance spectra for remote sensing data analysis must be undertaken with caution, even for targets such as cold deserts and polar regions which possess low weathering rates. Unweathered (interior) sample spectra may have little relevance to the field data being acquired. The bulk of the useful mineralogical information can be extracted from a few wavelength regions: near 1 μm, and between 2.15 and 2.6 μm. Fortunately, both lie outside the range of appreciable atmospheric absorption (Goetz et al. 1985). Further analysis of the laboratory data and compari-

sons with unweathered spectra may show systematic variations between these two classes of materials, and perhaps provide more information on the mechanism of cold desert weathering.

Acknowledgements. — This study was supported by a Grant-in-Aid for Northern Research from the Boreal Insitute for Northern Studies at the University of Alberta (#55-30274) and a Research Grant from the Geological Society of America (#3741-87). Thanks to Dr. Paul Lhotka, Dr. R. St J. Lambert, and Joan McCorquedale for providing the various samples. Special thanks to Dr. Bengt Lundén, Dr. Björn Sundquist and an anonymous reviewer for the many helpful comments and suggestions concerning this study.

References

Adams, J.B., 1975: Uniqueness of visible and near-infrared reflectance spectra of pyroxenes and other rock-forming minerals. *In* C. Karr (ed.): *Infrared and Raman spectroscopy of lunar and terrestrial minerals,* 91–116. Academic Press, N.Y.

Agresti, D.G., Morris, R.V., Newcomb, J.A. & Lauer, H.V. Jr., 1986: Spectral properties of selected soils from the dry valleys of Antarctica. *Lunar and Planetary Science Conference 17,* 3–4.

Anderson, L.W. & Anderson, D.S., 1981: Weathering rinds on quartzarenite clasts as a relative-age indicator and the glacial chronology of Mount Timpanogos, Wasatch Range, Utah. *Arctic and Alpine Research 13,* 25–31.

Bardin, V.I. & Konopleva, V.I., 1975: On the weathering process and the problem of geochronology of the glacial period. *In* V.A. Bugaev (ed.): *Antarctic Committee Report 1969,* 130–142. Amerind Publishing Co., New Delhi.

Bockheim, J.G., 1979: Relative age and origin of soils in eastern Wright Valley, Antarctica. *Soil Science 128,* 142–152.

Campbell, I.B. & Claridge, G.C.C., 1975: Morphology and age relationships of Antarctic soils. *Royal Society of New Zealand Bulletin 13,* 83–88.

Chinn, T.G.H., 1981: Use of rock weathering-rind thickness for Holocene absolute age-dating in New Zealand. *Arctic and Alpine Research 13,* 33–45.

Claridge, G.C.C., 1965: The clay mineralogy and chemistry of some soils from the Ross Dependency, Antarctica. *New Zealand Journal of Geology and Geophysics 8,* 186–220.

Clark, R.N., 1980: A large scale interactive one dimensional array processing system. *Publication of the Astronomical Society of the Pacific 92,* 221–224.

Clark, R.N., 1981: The spectral reflectance of water-mineral mixtures at low temperatures. *Journal of Geophysical Research 86,* 3074–3086.

Cloutis, E.A., 1985: *Interpretive techniques for reflectance spectra of mafic silicates.* M.Sc. thesis, University of Hawaii, 182 pp.

Glazovskaya, M.A., 1958: Weathering and primary soil formations in Antarctica. *Scientific Papers of the Institute of Geological and Geographical Sciences, Moscow University 1,* 63–76.

Goetz, A.F.H., Vane, G., Solomon, J.E. & Rock, B.N., 1985: Imaging spectrometry for earth remote sensing. *Science 228,* 1147–1153.

Hovis, W.A. Jr., 1965: Infrared reflecitivty of iron oxide minerals. *Icarus 4,* 425–430.

Hunt, G.R., 1977: Spectral signatures of particulate minerals in the visible and near infrared. *Geophysics 42,* 501–513.

Hunt, G.R., 1979: Near-infrared (1.3–2.4 μm) spectra of alteration minerals – Potential for use in remote sensing. *Geophysics 44,* 1974–1986.

Hunt, G.R. & Evarts, R.C., 1981: The use of near-infrared spectroscopy to determine the degree of serpentinization of ultramafic rocks. *Geophysics 46,* 316–321.

Hunt, G.R. & Hall, R.B., 1981: Identification of kaolins and associated minerals in altered volcanic rocks by infrared spectroscopy. *Clays and Clay Minerals 29,* 76–78.

Hunt, G.R. & Salisbury, J.W., 1970: Visible and near-infrared spectra of minerals and rocks: I Silicate minerals. *Modern Geology 1,* 283–300.

Hunt, G.R. & Salisbury, J.W., 1971: Visible and near-infrared spectra of mineals and rocks: II. Carbonates. *Modern Geology 2,* 22–30.

Hunt, G.R., Salisbury, J.W. & Lenhoff, C.J., 1971: Visible and near-infrared spectra of minerals and rocks: IV. Sulphides and sulphates. *Modern Geology 3,* 1–14.

Hunt, G. R., Salisbury, J. W. & Lenhoff, C.J., 1973*a*: Visible and near-infrared spectra of minerals and rocks: VI. Additional silicates. *Modern Geology 4,* 85–106.

Hunt, G.R., Salisbury, J.W. & Lenhoff, C.J., 1973*b*: Visible and near-infrared spectra of minerals and rocks: VII. Acidic igneous rocks. *Modern Geology 4,* 217–224.

Hunt, G.R., Salisbury, J.W. & Lenhoff, C.J., 1974: Visible and near-infrared spectra of minerals and rocks: IX. Basic and ultrabasic igneous rocks. *Modern Geology 5,* 15–22.

Jackson, M.L., Lee, S.Y., Ugolini, F.C. & Helmke, P.A., 1977: Age and uranium content of soil micas from Antarctica by the fission particle track replica method. *Soil Science 123,* 241–248.

Kelley, W.C. & Zumberge, J.H., 1961: Weathering of a quartz diorite at Marble Point, McMurdo Sound, Antarctica. *Journal of Geology 69,* 433–446.

King, T.V.V. & Ridley, W.I., 1987: Relation of the spectroscopic reflectance of olivine to mineral chemistry and some remote sensing implications. *Journal of Geophysical Research 92,* 11457–11469.

Lhotka, P.G., 1988: *Geology and geochemistry of gold-bearing iron formation in the Contwoyto Lake–Point Lake region, NWT, Canada.* PhD dissertation, University of Alberta, 265 pp.

Miyamoto, M., Mito, A., Takano, Y. & Fujii, N., 1981: Spectral reflectance (0.25–2.5 μm) of powdered olivines and meteorites, and their bearing on surface materials of asteroids. *Memoirs of the National Institute of Polar Research Special Issue 20,* 345–361.

Morris, R.V., 1985: Determination of optical penetration depths from reflectance and transmittance measurements on albite powders. *Lunar and Planetary Science Conference XVI,* 581–582.

Morris, R.V., Lauer, H.V. Jr., Lawson, C.A., Gibson, E.K. Jr., Nace, G.A. & Stewart, C., 1985: Spectral and other physicochemical properties of submicron powders of hematite (αFe_2O_3), maghemite (γFe_2O_3), magnetite (Fe_3O_4), goethite (α-FeOOH), and lepidocrocite (γ-FeOOH). *Journal of Geophysical Research 90,* 3126–3144.

Morris, R.V., Lauer, H.V. Jr., Agresti, D.G. & Newcomb, J.A., 1986: Spectral properties of "dust" produced in the dry valleys of Antarctica: A martian analogue? *MECA Workshop on Dust on Mars II (Lunar and Planetary Institute Technical Report 86–09),* 56–57.

Roush, T.L., Singer, R.B. & McCord, T.B., 1987: Reflectance spectra of selected phyllosilicates from .6 to 4.6 μm. *Lunar and Planetary Science Conference XVIII,* 856–857.

Sagan, C., Phaneuf, J.P. & Ihnat, M., 1965: Total reflection spectrophotometry and thermogravimetric analysis of simulated martian surface materials. *Icarus 4,* 43–61.

Sherman, D.M. & Waite, T.D., 1985: Electronic spectra of Fe^{3+} oxides and hydroxides in the near IR to near UV. *American Mineralogist 70,* 1262–1269.

Sherman, D.M., Burns, R.G. & Burns, V.M., 1982: Spectral characteristics of the iron oxides with application to the martian bright region mineralogy. *Journal of Geophysical Research 87,* 10169–10180.

Shipman, H. & Adams, J.B., 1987: Detectability of minerals on desert alluvial fans using reflectance spectra. *Journal of Geophysical Research 92,* 10391–10402.

Singer, R.B., 1981: Near-infrared spectral reflectance of mineral mixtures: Systematic combinations of pyroxenes, olivine, and iron oxides. *Journal of Geophysical Research 86,* 7967–7982.

Singer, R.B., 1982: Spectral evidence for the mineralogy of high albedo soils and dust on Mars. *Journal of Geophysical Research 87,* 10159–10168.

Singer, R.B., 1985: Spectroscopic observations of Mars. *Advances in Space Research 5,* 59–68.

Singer, R.B. & Blake, P.L., 1983: Effects of mineral grain size and physical particle size on spectral reflectance of basalts. *Lunar and Planetary Science Conference XIV,* 706–707.

Singer, R.B. & Roush, T.L., 1983: Spectral reflectance properties of particulate weathered coatings on rocks: Laboratory modeling and applicability to Mars. *Lunar and Planetary Science Conference XIV*, 708–709.

Tedrow, J.C.F., 1966: Polar desert soils. *Soil Science Society of America Proceedings 30*, 381–387.

Townsend, T.E., 1987: Discrimination of iron alteration minerals in visible and near-infrared reflectance data. *Journal of Geophysical Research 92*, 1441–1454.

Ugolini, F.C., 1966: Soil investigations in the lower Wright Valley, Antarctica. *NAS-NRC Publication 1278*, 55–61.

Ugolini, F.C., 1986: Process and rates of weathering in cold and polar desert environments. *In* S.M. Colman & D.P. Dethier (eds.): *Rates of chemical weathering of rocks and minerals*, 193–235. Academic Press, Orlando.

Ugolini, F.C. & Bull, C., 1965: Soil development and glacial events in Antarctica. *Quaternaria 7*, 251–269.

Vane, G. & Goetz, A.F.H. (eds.), 1985: *Proceedings of the Airborne Imaging Spectrometer Data Analysis Workshop*. JPL Publication 85–41, 173 pp.

Weidner, V.R. & Hsia, J.J., 1981: Reflection properties of pressed polytetrafluoroethylene powder. *Journal of the Optical Society of America 71*, 856–861.